Grain size effect on structural, electrical and mechanical properties of NiTi thin films deposited by magnetron co-sputtering

Ashvani Kumar [a,*], Devendra Singh [b], Davinder Kaur [a]

[a] Nanostructured Thin Films and Device Laboratory, Department of Physics, and Center of Nanotechnology, Indian Institute of Technology Roorkee, Roorkee-247667, India
[b] Metallurgy and materials Engineering Department, Indian Institute of Technology Roorkee, Roorkee-247667, India

ABSTRACT

In the present study NiTi films have been deposited on Si (100) substrates by dc magnetron co-sputtering in the temperature range from room temperature to 923 K. The crystallization, surface morphology and structural features were studied using X-ray diffraction (XRD), atomic force microscope (AFM), field emission scanning electron microscope (FESEM) and high resolution transmission electron microscope (HRTEM). In situ hot stage atomic force microscope was used to investigate the micro-structural changes during phase transformation in these films. Substrate temperature was found to have a great impact on the structural features and phase transformation behavior of NiTi films. The grain size and the crystallization extent increase with the increase in substrate temperature. Nanoindentation tests of these films were conducted at room temperature. Low hardness and depth recovery ratio was observed in case of the film deposited at substrate temperature of 923 K that could be due to the dominance of martensite phase at room temperature which results in more plastic deformation. The electrical properties of the films were studied using four probe resistivity method. Electrical resistance versus temperature plots show that grain size of NiTi films plays an important role in their electrical properties. NiTi based shape memory alloys exhibit a very interesting martensite to austenite phase transformation as crystal structure changes from monoclinic to cubic upon heating close to room temperature. The characteristics of this transformation are of immense technological importance due to a variety of MEMS applications.

© 2008 Elsevier B.V. All rights reserved.

1. Introduction

The shape memory effect and pseudoelastic behavior in intermetallic NiTi compound has been related to a crystallographic reversibility encountered during thermoelastic phase transformation. They display a unique inelastic strain recovery effect due to reversible first order thermal displacive transformation between low temperature monoclinic allotrope (martensite phase) to the high temperature cubic phase (austenite phase). Recent applications of NiTi alloys can be found in biomedical devices and various technological sectors [1–3].

Significant efforts have been devoted to explore the shape memory effect and pseudoelastic behavior of NiTi bulk. The effect of grain refinement over martensitic transformation in NiTi bulk has been reported by several research groups [4,5]. In spite of that the knowledge of such phenomenon in NiTi thin films is sparse. As a candidate material for microactuation, NiTi shape memory films have attracted renewed interest because of their fast response, competitively large transition forces, and a strain recovery rate comparable to

these of the bulk material [6,7]. Recent advances in semiconductors processing techniques and MEMS systems have turned the research attention to SMA thin films. Consequently, the systematic study is required to understand the associated phase transformation mechanism of NiTi thin films for scientific and industrial importance.

In the present study, NiTi thin films have been deposited by dc magnetron co-sputtering on Si (100) substrate at various substrate temperatures ranging from room temperature to 923 K. The magnetron sputtering has important specific advantages such as low levels of impurities and easy control of the deposition rate and also enables the production of thin films of various morphology and crystallographic structure. There are reports on composition effect, crystallization behavior, shape memory and pseudo elastic behavior, of dc sputtered NiTi thin films [8–14]. The aim of the present study was to examine the effect of grain size on the crystallinity, surface morphology and phase transformation behavior of NiTi thin films. It was observed that the martensitic transformation behavior of these films depends critically on its microstructure and its dimensional constraint. The NiTi film deposited at substrate temperature (T_s) of ≤623 K exhibited negative thermal coefficient of resistance (TCR) value and non-metallic behavior, while the film deposited at T_s of ≥723 K showed metallic behavior.

* Corresponding author.
  E-mail address: kashudmt@iitr.ernet.in (A. Kumar).

2. Experimental details

NiTi films were deposited on (100) silicon substrate at various substrate temperatures by dc magnetron sputtering system. The substrates were initially cleaned thoroughly in an ultrasonic bath with a mixture of distilled water and trichloroethylene in 4:1 ratio and then washed with boiled acetone. High purity (99.99%) titanium and nickel metal targets of 50 mm diameter and 3 mm thickness were used. Before every sputtering run, the targets have been pre-sputtered for 5 min in order to ascertain the same state of the targets in every run. Suitable powers were applied to each target to give similar deposition rates of Ni and Ti. Substrate holder was rotated axially at 2 rpm to achieve a uniform film composition. Both magnetron guns were tilted at an angle of 45° so that the plasma from both the targets can be concentric. The Ti/Ni ratio was determined from energy dispersive X-ray analysis (EDAX). Before sputtering deposition, the chamber was evacuated to a base pressure of the order of 10^{-7} Torr and then backfilled with argon to the desired pressure. The chamber pressure was measured using a combination vacuum gauge (Pfeiffer Vacuum). The target to substrate distance was fixed at approximately 5 cm. The films were deposited for 30 min in the temperature range from room temperature to 923 K. The film thickness was measured using a surface profilometer and cross sectional FESEM and was found to vary from 2.2 to 2.5 µm with increase in substrate temperature from 623 to 923 K. Post annealing was not performed after deposition.

The orientation and crystallinity of the films were studied using a Bruker advanced diffractometer of CuKα (1.54 Å) radiations in θ–2θ geometry at a scan speed of 1°/min. To make sure of absolute values of the 2θ diffraction angles, the diffractometer was calibrated with respect to the peak position of an Si calibration standard. A polycrystalline powder was used for instrumental correction. The coherently diffracting domain size (d_{XRD}) was calculated from the integral width of the diffraction lines using the Scherrer's equation [15], after background subtraction and correction of instrumental broadening. The surface topography and microstructure were studied using field emission scanning electron microscope (FEI Quanta 200F) and atomic force microscope (NT-MDT: NTEGRA Model). The microstructure was also investigated using high resolution transmission electron microscopy (HRTEM). The resistivity of the films was measured by four probe resistivity method using a liquid nitrogen cryocooler and Keithley instruments over a temperature range from 100 to 400 K. The contacts over the samples were made by silver paint.

A Hysitron Triboindenter was used to perform nanoindentation tests. Sixteen nanoindentation tests were performed on each sample using a diamond Berkovich indenter probe to determine the hardness
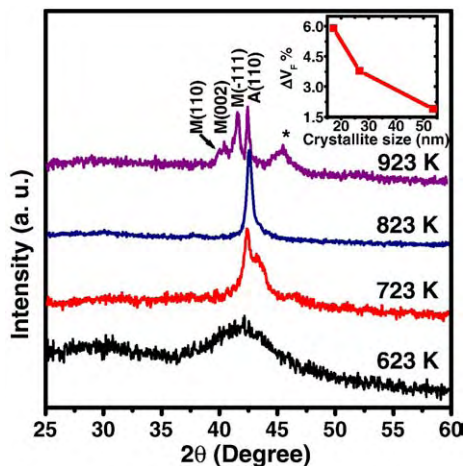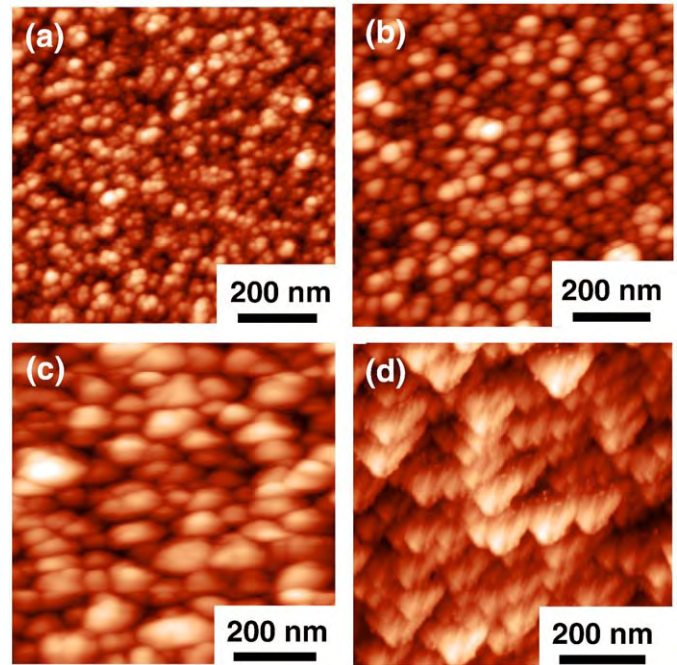

Fig. 2. AFM images of NiTi films deposited at T_s of (a) 623 K, (b) 723 K, (c) 823 K and (d) 923 K.

and reduced modulus. Each test consisted of a five-second linear loading segment to a peak load, followed by a two-second holding segment at the peak load, and finally a five-second linear unloading segment. The maximum load was set at 3.5 mN so that indentation would not exceed 10% of the film thickness in order to minimize the substrate influence on the indentation response of the films.

3. Results and discussion

3.1. Structural properties

The martensite transformation and superplasticity of NiTi films are sensitive to the deposition temperature, post-annealing temperature and duration [16,17]. The films deposited at room temperature were usually amorphous in nature. Therefore high temperature deposition or post annealing was required to make them crystalline. It is suggested that postannealing should be done at the lowest possible annealing temperature for minimum annealing duration to minimize the reaction between film and substrate otherwise it could lead to dramatic changes in the film microstructure, mechanical properties and shape memory effects [16]. An alternative method to avoid high temperature treatment is to grow the NiTi thin films on heated substrates during deposition. The films deposited at relatively higher substrate temperature (≥723 K) do not require post annealing and these are in situ crystallized [18]. In order to see the impact of substrate temperature on microstructural and phase transformation behavior of NiTi films, various films were prepared at different substrate temperature and no post annealing was performed on these films.

Fig. 1 shows the XRD pattern of NiTi films deposited at substrate temperatures of 623, 723, 823 and 923 K. The NiTi film deposited at substrate temperature (T_S) of 623 K was amorphous in nature while the film deposited at T_s of 723 and 823 K exhibited the reflection from (110) plane of the austenite parent phase structure. This showed that crystallization starts in NiTi films grown onto Si (100) substrate at the deposition temperature as low as 723 K. XRD pattern confirmed that the dominant phase at room temperature was austenite in the film

**Fig. 1.** XRD pattern of NiTi films deposited at T_s of 623 K, 723 K, 823 K and 923 K.

Table 1
Various parameters of NiTi films deposited at T_s of 623 K, 723 K, 823 K and 923 K

Sample number	Substrate temperature (T_s)	Grain size (nm)				Avg. roughness (nm)	EDAX at. wt.% Ti: Ni
		XRD along (110) peak	FESEM	TEM	AFM		
1.	623 K	–	21.7	20.1	22.2	3.87	49.7:50.3
2.	723 K	17.2	38.3	33.6	39.6	6.75	49.9:50.1
3.	823 K	26.7	77.7	67.0	80.0	8.12	50.2:49.8
4.	923 K	53.4	108.2	98.2	112.5	23.4	50.6:49.4

deposited at T_s of ≤823 K while the film deposited at T_s of 923 K showed sharp peak of (−111) reflection at $2\theta = 41.7°$ and other less intensity peaks of (002) and (110) reflections correspond to mono-clinic martensitic structure (Fig. 1). Increase in substrate temperature from 623 K to 823 K enhanced activity of absorbed atoms on the substrate and accelerates the migration of the atoms to the favorable energy positions that favors to the formation of closed packed structure to reduce the surface energy of the grown film which lead to development of the strong (110) plane texture. Moreover, the rapid crystallization of sputtered atoms would confine the crystallized grains within a very small size. Further increase in substrate temperature, above eutectoid temperature of NiTi compound ($T_e = 903$ K) [19], would facilitate small grains to be aggregated and grow, which could be responsible for the dominance of martensitic phase at room temperature in the NiTi film deposited at T_s of 923 K. The mean crystallographic domain size or particle size was estimated from the true broadening of the XRD lines, using the Sherrer's formula [15]. Estimated average crystallite size of the films deposited at 723, 823 and 923 K was found to be 17.2, 26.7 and 53.4 nm, respectively corresponding to the (110) peak broadening of austenitic phase.

The surface morphology of these films was analyzed using atomic force microscopy and is shown in Fig. 2. AFM micrographs revealed
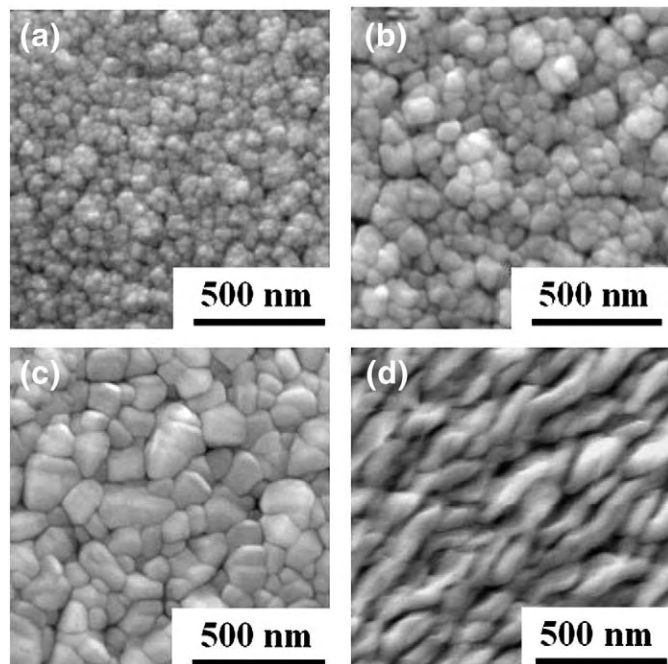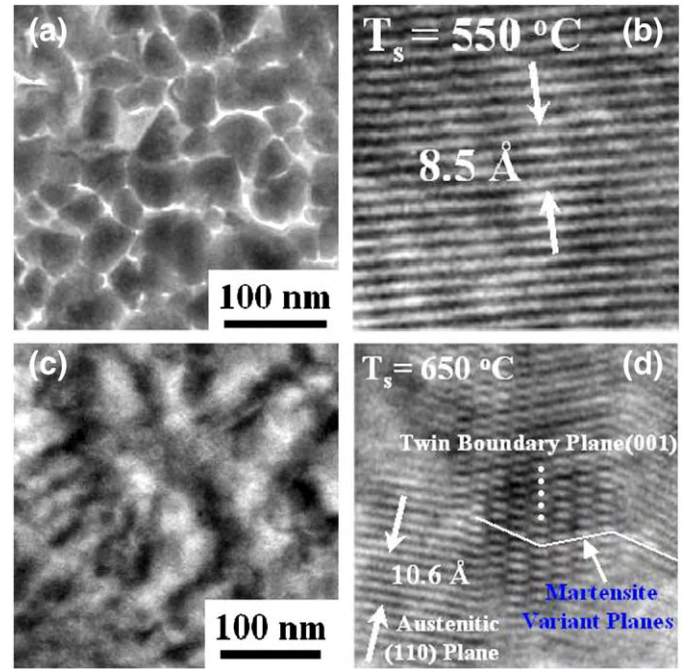
Fig. 4. TEM micrographs of NiTi film deposited at T_s of (a) 823 K and (c) 923 K; High resolution lattice images of NiTi film deposited at T_s of (b) 823 K and (d) 923 K.

that the NiTi film deposited at 723 and 823 K shows non facets grains (Fig. 2(b) and (c)) with average surface roughness of 6.75 and 8.12 nm, respectively while facets with preferential in-plane orientation of martensitic phase (martensitic plates) (Fig. 2(d)) was observed for the film deposited at 923 K. It was observed that the grain size increases with increase in substrate temperature, which was in agreement with the XRD results as reported in Table 1. It has been proposed that the grain boundaries impose constraints on the growth of the martensite and confine the transformed volume fraction in the nanocrystalline structure. A martensite plate nucleated within a grain will be stopped at the grain boundaries acting as obstacles for martensite growth. To propagate the transformation, the plate has to exert stresses that are sufficient to stimulate nucleation and growth of favorable martensite variants in the adjacent grains [20]. In order to estimate the density of grain boundaries, the excess free volume associated with the grain boundaries were calculated using the following expression [21]:

$$\Delta V_F = \frac{(L + d/2)^2 - L^2}{L^2}.$$

Where L is the crystallite size and d is the mean width of the grain boundaries. In most of the prior calculations of the excess free volume, the width of the grain boundary has been assumed to be constant ($d = 1$ nm), independent of the grain size. The variation of excess free volume with crystallite size has been shown in the inset of Fig. 1. It was observed that the grain boundary free volume increases with decrease in crystallite size, hence, grain boundaries increases with decrease in crystallite size. Also, with the decrease in grain size, the number of grain boundaries per unit area and the number of boundary interfaces increase.

Fig. 3(a) to (d) shows the FESEM micrographs that clearly resolved the change of microstructure of NiTi thin films deposited at substrate temperatures of 623, 723, 823 and 923 K respectively. The grain size of these films was estimated using FESEM micrographs, which clearly revealed the increase in grain size with increase in substrate temperature as reported in Table 1. A slight change in film composition was observed with change in substrate temperature. Atomic weight
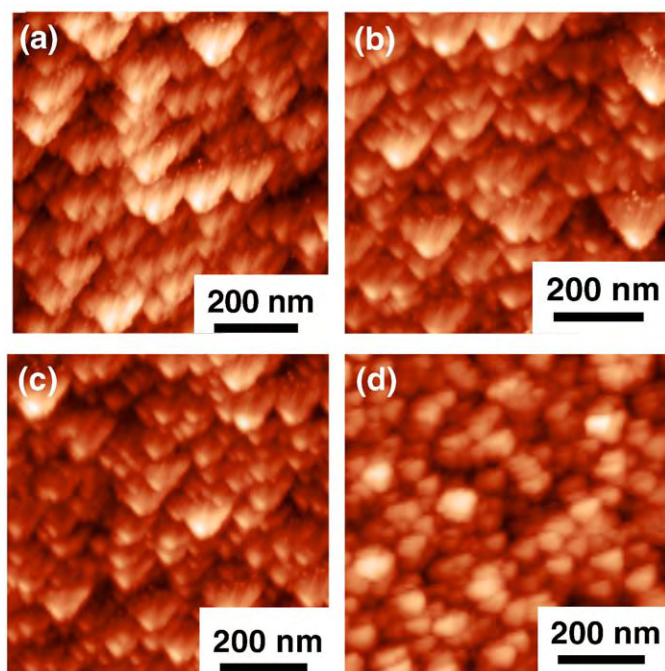

Fig. 3. FESEM images of NiTi films deposited at T_s of (a) 623 K; (b) 723 K; (c) 823 K and (d) 923 K.

Fig. 5. Hot stage AFM images of NiTi films deposited at T_s of 923 K at different temperatures (a) 298 K, (b) 328 K, (c) 358 K and (d) 388 K.

percentage of Ni and Ti in these films is reported in Table 1. The microstructure of these films was also investigated using high-resolution transmission electron microscopy (HRTEM) at electron beam energy of 200 KeV. Fig. 4(a) and (c) shows the TEM micrographs of the NiTi film deposited at substrate temperature of 823 and 923 K respectively, which are in agreement with the FESEM and AFM results. High-resolution lattice images of these films are shown in Fig. 4(b) and (d). In case of the film deposited at the substrate temperature of 823 K, the lattice image shows a lattice spacing of 2.12 Å, which is in the agreement with the 'd' spacing of (110) plane of austenitic phase (Fig. 4(b)). Fig. 4(d) shows the lattice image of the film deposited at T_s=923 K, which revealed the mixed phase i.e. d spacing of 2.12 Å corresponds to (110) plane of austenitic phase and the compound twins of (001) plane yielding a minimum width of four lattice planes (8.5 Å) exhibited martensitic phase.

To gain further insight, hot stage in situ atomic force microscopy was used in order to investigate the surface morphology transition between austenite and martensite phase as a function of temperature. The sample was pre-cooled by liquid nitrogen below a temperature of 250 K, and then heated back to room temperature in atmosphere. Fig. 5(a)–(d) shows the two dimensional surface morphology of the NiTi film deposited at 923 K with increasing temperature i.e. 298, 328, 358 and 388 K, respectively. Each measurement was made after the temperature was stabilized. With increase in temperature the martensitic plate like structure starts to disappear and completely dissolved in to the background at the temperature of 373 K, which confirmed the phase transformation between martensite and austenite phase. The root mean square (rms) roughness quantitatively identifies the surface roughness of these films. In the subsequent heating/cooling cycle, surface roughness of the scanned area was measured in-between the temperature range from 298 to 388 K with step size of 15 K as shown in Fig. 6. The surface roughness of the martensite phase was found to be much higher as compared to that of austenite phase. As the temperature increases, the surface roughness decreases drastically that clearly confirm the phase transformation between martensite and austenite phases.

3.2. Electrical properties

Matthiessen's rule states that the total electrical resistance of an alloy is the sum of the resistance due to electron scattering by phonons and the resistance due to electron scattering because of lattice imperfections and impurities. Phase transformation affects the density of lattice imperfection, therefore, electrical resistance versus temperature response provides an effective means for detecting the formation of various phases in shape memory alloys.

The resistances versus temperature (R–T) plots of NiTi films grown at various substrate temperatures are shown in Fig. 7 and corresponding transformation temperatures are reported in Table 2. The temperature dependence of electrical resistance was measured in the temperature range of 100–400 K during subsequent heating and cooling cycles. The R–T plot of the film deposited at T_s of 623 K (Fig. 7(a)) exhibited nonmetallic behavior with negative thermal coefficient of resistance (TCR) value (Fig. 8(a)). The observed behavior could be attributed to the following reasons: (a) due to the presence of intrinsic defects [22]; (b) Austenite↔R-phase transition that can occur in the amorphous-nanocrystalline alloys [23]. During cooling, self accommodation R-phase transformation commenced at temperature of 300 K and austenite parent phase began to transform to the twinned R-phase with further decrease in temperature. Cooling of the sample even up to 150 K resulted only in R-phase transformation. Both the lattice distortion and twinning are reversible process in R-phase transformation, therefore, R–T plots do not exhibit temperature hysteresis [Fig. 7(a)].

With increasing substrate temperature, the progressive crystallization of the samples induced an evident diminishing of the intrinsic defect, which yields the resistance versus temperature behavior to change from nonmetallic (observed in amorphous NiTi film deposited at T_s=623 K) to metallic regime (in case of crystalline films deposited at T_s=723, 823 and 923 K). NiTi films deposited at 723 K exhibited metallic like behavior without any indication of phase transformation in between martensitic and austenitic phases (Fig. 7(b)). The suppression of phase transformation phenomenon could be due to the very small grain size causing higher number of grain boundary interfaces and associated excess free volume as shown in inset of Fig. 1. As the constraints imposed by the grain boundaries on the growth of martensite confined the transformed volume fraction in the nano grained structures and hence could lead to suppression of martensitic transformation in nanocrystalline NiTi thin films. Fig. 8(b) shows TCR versus temperature plot of the film deposited at T_s of 723 K. An abrupt behavior of TCR was observed in the temperature range from 266 to 400 K during subsequent heating and cooling cycles, which clearly
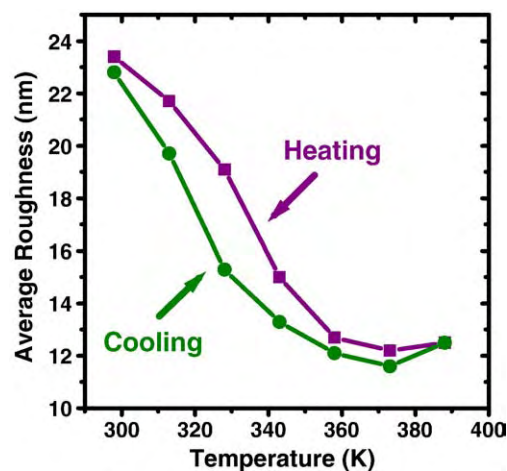

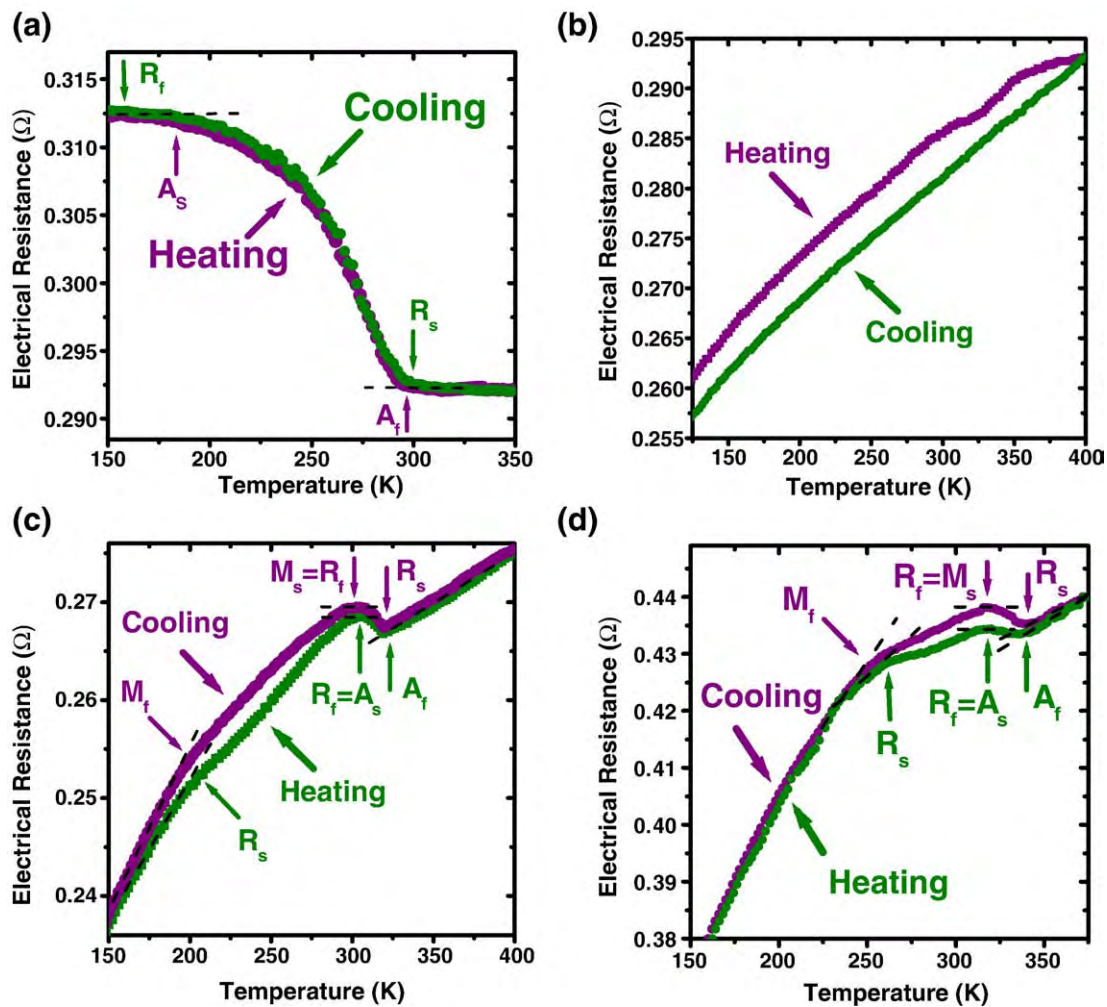**Fig. 6.** Surface roughness versus temperature plot.

Fig. 7. Electrical resistance versus temperature curve of NiTi films deposited at T_s of 623 K, (b) 723 K, (c) 823 K and (d) 923 K.

shows incomplete phase transformation due to constraints imposed by grain boundaries.

Fig. 7(c) shows the *R–T* plot of NiTi thin film deposited at 823 K that clearly indicates the phase transformation from martensite to austenite phase and vice versa via R-phase during subsequent heating and cooling cycles. A linear decrease in electrical resistance with temperature was observed during cooling from 400 K because of the decreasing intensity of electron–photon interactions. At temperature R_s (318 K), the austenite phase is distorted and starts to transform to R-phase. The formation of R-phase during phase transformations could be attributed to the fact that in small grains, the constraints of grain boundaries exhibited significantly small shape strain (~1%) during transformation from austenitic to R-phase as compared to 10% in case of austenitic to martensitic phase [24]. The decrease in strain by twinning plays an important role in R-phase formation because it proceeds by nucleation and growth in parent phase in a hetero-geneous manner. Therefore, R-phase formation is a self accommoda-tion process, which occurs gradually in the parent phase with the decrease of temperature. Electron scattering by lattice imperfection become pronounced as compared to the electron scattering by phonon with decrease in temperature below 318 K. This is because of increased density of twinned structure that results in the increase of electrical resistance. The cooling of the sample below R_f (304 K) promotes R-phase to martensite transformation, which exhibit less lattice distortion with no additional twinning. The electrical resistance was observed to decrease below temperature R_f [Fig. 7(c)] which may be due to less electron scattering by lattice distortion.

Martensite transformation gets complete below the temperature M_f. During the heating cycle, the electrical resistance almost follows the same trend as obtained during cooling. Detwinning in this film commenced as the temperature increases to austenite start tempera-ture (A_s). R-phase to austenite transformation is completed at temperature A_f (320 K) and NiTi microstructure completely reverses to the single cubic austenite microstructure. *R–T* curves showed that in small grained NiTi film, transformation processes take place according to the following procedures:

Martensite↔R − phase↔austenite(during heating and cooling)

The values of M_s (martensite start temperature) and A_f (austenite finish temperature) were found to be 304 K and 320 K for the film deposited at T_s of 823 K.

Table 2
Details of transformation temperatures obtained from electrical resistance versus temperature curves of NiTi films deposited at T_s of 623 K, 723 K, 823 K and 923 K

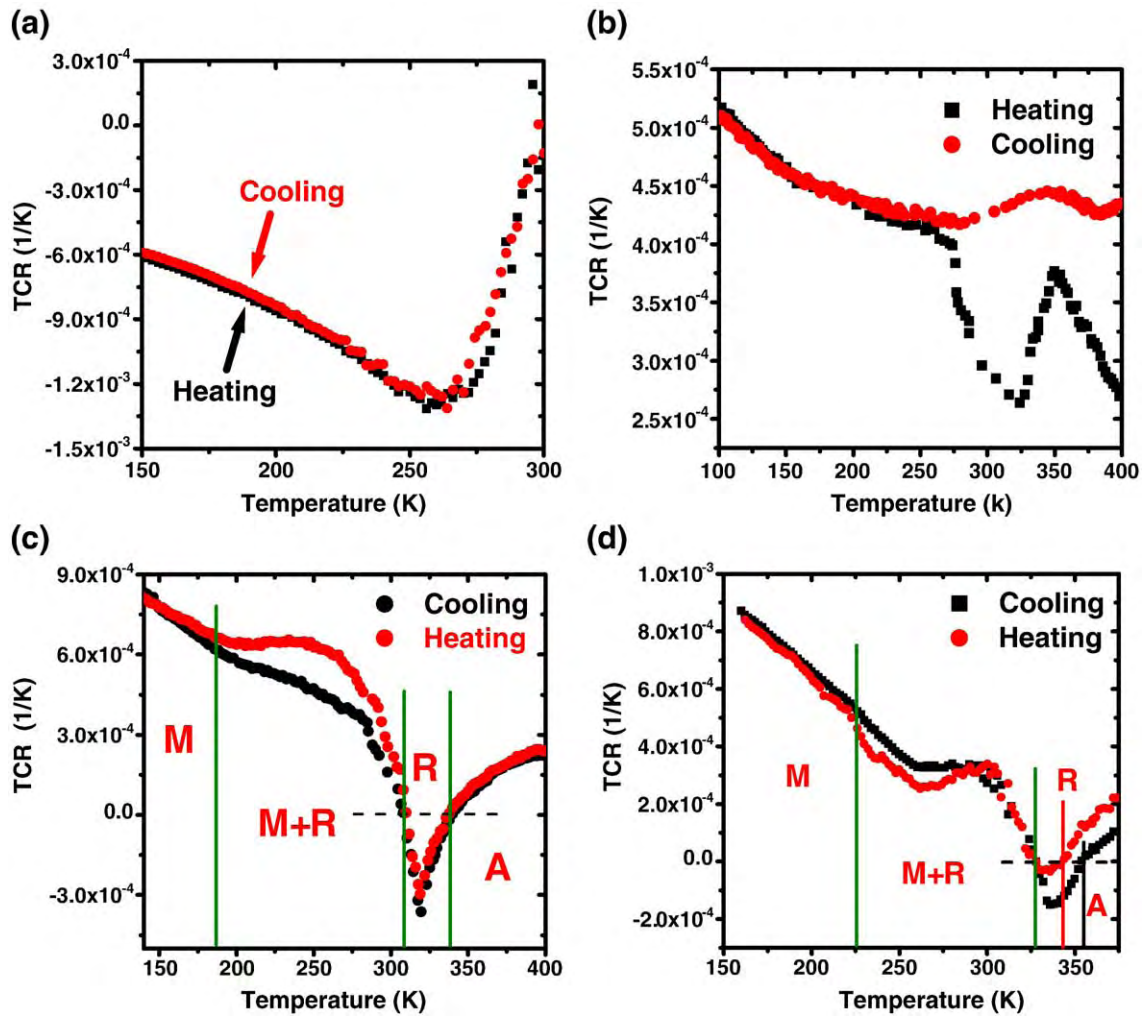| Sample number	Substrate temperature (T_s)	Transformation temperature (K)						Hysteresis width (K)
		Heating			Cooling			
		R_s	$R_f=A_s$	A_f	R_s	$R_f=M_s$	M_f	
1.	823 K	208	302	320	318	304	200	18
2.	923 K	260	319	341	339	316	252	24

Fig. 8. Thermal coefficient of resistance versus temperature curve of NiTi films deposited at T_s of (a) 623 K, (b) 723 K, (c) 823 K and (d) 923 K.

Fig. 8(c) displays the thermal coefficient of resistance versus temperature plot of the film deposited at T_s of 823 K for subsequent heating and cooling cycles. During heating cycle initially, a linear decrease in TCR value was observed with increasing temperature and thereafter a sharp decrease was observed with a transition from positive to negative value at 310 K. The TCR value remained negative in the temperature range of 310 K–338 K with a peak at 318 K. The observed continuous and sharp changes from positive to negative value of TCR could be due to the fast growth of R-phase because the TCR is found to be negative in R-phase. With further increase in temperature above 330 K, the TCR again become positive, which indicates R-phase to austenite parent phase transformation. Similar behavior of TCR was observed during cooling cycle. Therefore the observed variation in TCR as a function of temperature confirmed martensite↔R-phase↔austenite phase transformations during heating and cooling cycles.

Fig. 7(d) shows the electrical resistance response of the NiTi film deposited at 923 K. The behavior of the R–T curves was found to be similar with the observed for the film deposited at 823 K except that the martensite start temperature (316 K) and austenitic final temperature (341 K) were found to be shifted towards higher temperature range. This could be due to the dominance of martensitic phase at room temperature. TCR versus temperature curves exhibited positive to negative transition and vice versa for subsequent cooling and heating cycles as showed in Fig. 8(d). A remarkable difference was observed in the peak value of TCR i.e. -1.5×10^{-4} and -2.7×10^{-5} during

cooling and heating cycles, respectively. The low peak value and slope of TCR curve during heating cycle indicated the suppression of R-phase that could be due to the presence of martensite and R-phase in the matrix at 334 K.
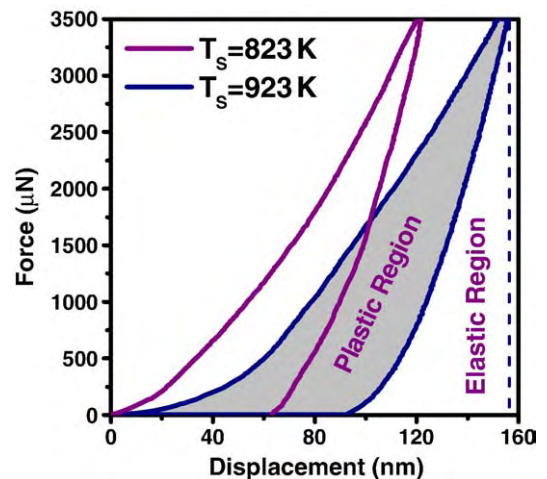

Fig. 9. Load–displacement curve of NiTi films deposited at T_s of 823 K and 923 K.

3.3. Mechanical properties

Fig. 9 shows the load–displacement curve for the films deposited at 823 and 923 K. Hardness, reduced modulus, indent depth recovery ratio, dissipation energy and wear behavior of the films deposited at T_s of 823 and 923 K have been evaluated by using load–displacement curves in order to reveal the qualitative behavior for the two crystallographic states. Fig. 10 shows the variation of hardness with contact depth for both samples. The average hardness of NiTi films exhibited austenite phase (deposited at T_s=823 K) and dominant martensite phase (deposited at T_s=923 K) at room temperature was observed 7.3±0.6 and 4.8±0.8 respectively, beyond a contact depth of ~70 nm. The hardness value showed that the austenite phase has more hardness as compared to that of martensite phase.

The indentation induced super elasticity effect can be characterized by the depth recovery ratio from the load versus depth curves by using the following equation [14]:

$$\text{Depth Recovery Ratio} = \frac{h_{\max} - h_r}{h_{\max}}$$

Where $h_{\max}$ is the penetration depth at the maximum load and h_r is the residual depth when the load returns to zero during unloading. The depth recovery ratio of the films deposited at T_s of 823 and 923 K was found to be 0.48 and 0.40, respectively. Lower depth recovery ratio (0.4) was observed for the film deposited at T_s of 923 K. This could be due to the dominance of martensite phase at room temperature that deformed easily by the reorientation of the martensite variants.

The dissipation energy (W_D) was evaluated from numerical integration of the area between the loading and unloading curves caused by dislocation movement, martensite transformation and martensite reorientation [25,26]. Dissipation energy of film exhibited martensite state at room temperature was found to be more as compared to the film showed austenite state that could also be due to the easy deformation of martensitic phase than that of austenite phase (Fig. 11).

The average hardness (H) and reduced elastic modulus (E_r) were calculated for both samples from indentation load versus depth curves. Hardness (H) to Young modulus (E) ratio has been proposed as the key factor to measure the behavior of wear resistance of the thin film coatings. It has been reported that the deformation around the indenter surface exhibit piling-up and sinking-in and the tendency of
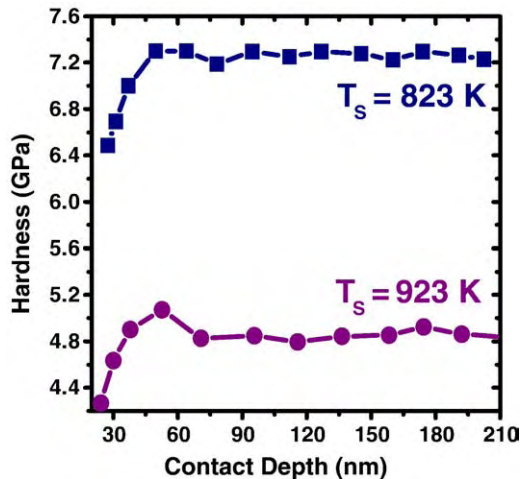

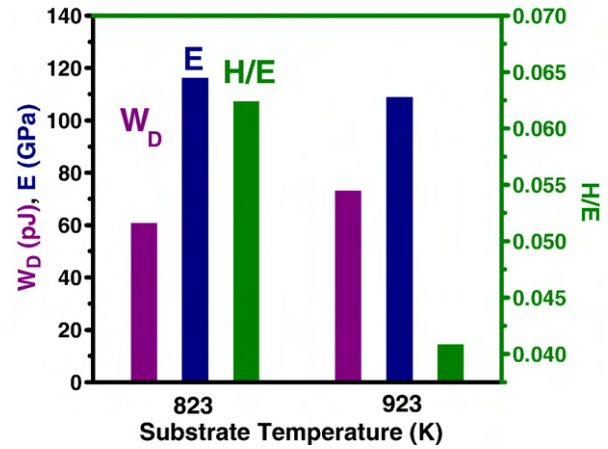**Fig. 11.** Dissipation energy (W_D), reduced modulus (E_r) and hardness to reduced modulus ratio (H/E) of NiTi films deposited at T_s of 823 K and 923 K.

sinking-in increases with increasing H/E ratio [27]. Fig. 11 shows the plot of H/E ratio of NiTi films deposited at 823 and 923 K. A relative low value of H/E ratio (0.04) for NiTi film exhibited martensite phase at room temperature indicated that more fraction of work is consumed in plastic deformation and large plastic strain is expected when contacting a material. Higher value of H/E ratio in case of the film exhibited austenite phase at room temperature is expected to have smaller accumulative strain and strain energy results relatively better wear resistance.

4. Conclusions

In summary, NiTi thin films were grown on Si (100) substrate by dc magnetron sputtering in the temperature range from room temperature to 923 K. Substrate temperature was found to have a great impact on surface morphology, crystallite size, mechanical properties and phase transformation behavior of these films. XRD pattern showed that the film deposited at T_s of 623 K was amorphous in nature while the film deposited at 723 K and 823 K exhibited the reflection from (110) plane of the austenite phase. With further increase in deposition temperature to 923 K, reflection from (−111), (002) and (110) planes of martensite structure was observed. Surface morphology of these films was found to change from non facet grains to facet grains with preferential in-plane orientation (martensite plates) with change in substrate temperature from 823 K to 923 K. The NiTi film deposited at substrate temperature (T_s) of ≤623 K exhibited negative TCR value and non-metallic behavior while the film deposited at T_s of ≥723 K showed metallic behavior. Electrical resistance versus temperature curves conformed that in a volume containing many small grains, the ability of phase transformation due to autocatalytic nucleation decreases with increase in grain boundary area. Nanoindentation studies revealed relatively low surface roughness, high hardness, high reduced elastic modulus and better wear behavior for the film exhibited austenitic structure at room temperature in comparison to that exhibited martensitic structure.

Fig. 10. Hardness versus contact depth curves of NiTi films deposited at T_s of 823 K and 923 K.

References

[1] J.V. Hunbeek, Mater. Sci. Eng., A 134 (1999) 273.
[2] A. Ishida, V. Martynov, MRS Bull. 27 (2002) 111.
[3] Q. Pan, C. Cho, Sensors 7 (2007) 1887.
[4] X. Xu, N. Thadhani, Scr. Mater. 44 (2001) 2477.
[5] R.Z. Valiev, J. Mater. Sci. 42 (2007) 1483.
[6] J.J. Gill, D.T. Chang, L.A. Momoda, G.P. Carman, Sens. Actuators, A, Phys. 93 (2001) 148.
[7] J.V. Humbeck, Adv. Eng. Mater. 3 (2001) 837.
[8] F.F. Gong, H.M. Shen, Y.N. Wang, Mater. Lett. 25 (1995) 13.
[9] F.F. Gong, H.M. Shen, Y.N. Wang, Appl. Phys. Lett. 69 (1996) 2656.
[10] Y.Q. Yang, H.S. Jia, Z.F. Zhang, H.M. Shen, A. Hub, Y.N. Wang, Mater. Lett. 22 (1995) 137.
[11] J.D. Busch, A.D. Johnson, C.H. Lee, D.A. Stevenson, J. Appl. Phys. 68 (1990) 6224.
[12] K.R.C. Gisser, J.D. Busch, A.D. Johnson, A.B. Ellis, Appl. Phys. Lett. 61 (1992) 1632.
[13] E. Wibowo, C.Y. Kwok, J. Micromechanics Microengineering 16 (2006) 101.
[14] Y. Zhang, Y.T. Cheng, D.S. Grummon, J. Appl. Phys. 98 (2005) 033505.
[15] B.D. Cullity, Elements of X-ray Diffraction, Addison-Wesley, Reading, MA, 1970, p. 102.
[16] Y. Fu, H. Du, W. Huang, S. Zhang, M. Hu, Sens. Actuators, A 112 (2004) 395.
[17] H.J. Lee, H. Ni, D.T. Wu, A.G. Ramirez, Appl. Phys. Lett. 87 (2005) 114102.
[18] Y. Fu, H. Du, Mater. Sci. Eng., A 236 (2003) 322.
[19] J.L. Murray (Ed.), Phase Diagrams of Binary Titanium Alloys, ASM International Metals Park, 1987.
[20] T. Saburi, S. Nenno, in: I. Tamura (Ed.), Proceedings of the International Conference on Martensitic Transformations, Japan: The Japan Inst Metals, Japan, 1986, p. 671.
[21] R. Banerjee, E.A. Sperling, G.B. Thompson, H.L. Fraser, S. Bose, P. Ayyub, Appl. Phys. Lett. 82 (2003) 4250.
[22] M.A. Arranz, J.M. Riveiro, J. Magn. Magn. Mater. 290–291 (2005) 865.
[23] V.G. Pushin, R.Z. Valiev, Solid state phenomena 94 (2003) 13.
[24] T. Waitz, V. Kazykhanov, H.P. Karnthaler, Acta Mater. 52 (2004) 137.
[25] K. Komvopoulos, X.G. Ma, Appl. Phys. Lett. 87 (2005) 263108.
[26] K. Gall, K. juntunen, H.J. Maier, H. Sehitoglu, Y.I. Chumlyakov, Acta Mater. 49 (2001) 3205.
[27] W. Ni, Y.T. Cheng, M.J. Lukitsch, A.M. Weiner, L.C. Lev, D.S. Grummon, Appl. Phys. Lett. 18 (2004) 4028.